Selective cadmium fluorescence probe based on bis-heterocyclic molecule and its imaging in cells

Masayori Hagimori (hagimori@mukogawa-u.ac.jp)
Mukogawa Women's University: Mukogawa Joshi Daigaku https://orcid.org/0000-0002-2371-911X
Yasushi Karimine
Nagasaki University: Nagasaki Daigaku
Naoko Mizuyama
Translational Research Center for Medical Innovation
Fumiko Hara
Mukogawa Women's University: Mukogawa Joshi Daigaku
Takeshi Fujino
Saitama University Graduate School of Science and Engineering: Saitama Daigaku Daigakuin Rikogaku Kenkyuka
Hideo Saji
Kyoto University Graduate School of Pharmaceutical Sciences Faculty of Pharmaceutical Sciences: Kyoto Daigaku Daigakuin Yakugaku Kenkyuka Yakugakubu
Takahiro Mukai
Kobe Pharmaceutical University: Kobe Yakka Daigaku

Research Article

Keywords: Cd2+, Fluorescent probe, Bis-heterocyclic molecule, Low-molecular-weight, Cell membrane permeability

Posted Date: March 26th, 2021

DOI: https://doi.org/10.21203/rs.3.rs-260927/v1

Version of Record: A version of this preprint was published at Journal of Fluorescence on May 13th, 2021. See the published version at https://doi.org/10.1007/s10895-021-02748-7.

Abstract

Fluorescence probes that selectively image cadmium are useful for detecting and tracking the amount of Cd^{2+} in cells and tissues. In this study, we designed and synthesized a novel Cd^{2+} fluorescence probe based on the pyridine-pyrimidine structure, 4-(methylsulfanyl)-6-(pyridin-2-yl)pyrimidin-2-amine (**3**), as a low-molecular-weight fluorescence probe for Cd^{2+}. Compound **3** could successfully discriminate between Cd^{2+} and Zn^{2+} and exhibited a highly selective turn-on response toward Cd^{2+} over biologically related metal ions. The dissociation constant and detection limit of 5.4×10^{-6} mol L^{-1} and 4.4×10^{-7} mol L^{-1}, respectively, were calculated using fluorescence titration experiments. Studies with closely related analogs showed that the bis-heterocyclic moiety of **3** acted as both a coordination site for Cd^{2+} and a fluorophore. Further, the methylsulfanyl group of compound **3** is essential for achieving selective and sensitive Cd^{2+} detection. Fluorescence microscopy studies using living cells revealed that the cell membrane permeability of compound **3** is sufficient to detect intracellular Cd^{2+}. These results indicate that novel bis-heterocyclic molecule **3** has considerable potential as a fluorescence probe for Cd^{2+} in biological applications.

Introduction

Cadmium, a toxic heavy metal that occurs naturally in soils and minerals, can accumulate in rice and vegetables through soil-to-plant transference [1,2]. The uptake of cadmium by food is unavoidable and causes serious health problems, especially in kidneys, lungs, liver, and the nervous system [1,3–5]. In addition, long-term exposure to cadmium is considered a causative factor in lung, prostate, breast, and kidney cancers because of its long biological half-life in humans (17–30 years) [3,6–8]. Therefore, reliable methods that can detect cadmium in living cells and tissues are urgently required.

To investigate heavy metal ions including Cd^{2+} in living systems, several analytical methods, such as atomic absorption spectrometry and inductively coupled plasma (ICP) mass spectrometry, have been commonly used [9,10]. These methods are suitable for measuring the total metal ion content in tissues, but unsuitable for real-time monitoring in specific cells or tissues. Alternatively, organic fluorescence probes are useful for real-time detection and tracking trace amounts of metal ions in living systems because of their selectivity and sensitivity. Further, their fluorescence properties can be tuned for targeting metal ions by chemical modification, which is an added advantage [11,12]. There have been efforts to develop Cd^{2+}-selective fluorescence probes consisting of a metal coordination site and fluorophore [13–18]; however, only a few are available owing to their poor selectivity, solubility, or cell membrane permeability. More importantly, the inability to distinguish between Zn^{2+} and Cd^{2+} is a critical issue and hinders the development of Cd^{2+}-selective fluorescence probes [13-16]. Zn^{2+} and Cd^{2+} exhibit comparable physical and chemical properties because they belong to the same group in the periodic table [12]; therefore, only a few probes that successfully discriminate Zn^{2+} and Cd^{2+} have been reported [17,18]. Although chemical modification is an effective method to overcome this issue, it yields a high molecular

weight compound with a complex chemical structure. Consequently, the cell membrane permeability of fluorescence probes worsens.

Bis-heterocyclic compounds such as 2,2′-bipyridine are known as chelating ligands that form charge complexes with several types of metal ions and are used as core structures for drug-like molecules and fluorescence probes [19-22]. Previously, bis-heteroaryl core structures, which acted as the coordination site for Zn^{2+} and fluorophores, have been exploited as low-molecular-weight fluorescence probes for Zn^{2+} [23-25]. These probes based on the bis-heteroaryl core had molecular weights of less than 500 g mol^{-1}, which showed clear chelation enhanced fluorescence (CHEF) effect on target metal ions and enabled good cell membrane permeability. In addition, a simple tuning of the electron density of the core structure by introducing electron-donating or electron-withdrawing groups greatly affected the intermolecular charge transfer (ICT) state and metal selectivity including Cd^{2+}.

Herein, we have designed and synthesized a novel low-molecular-weight Cd^{2+} fluorescence probe (4-(methylsulfanyl)-6-(pyridin-2-yl)pyrimidin-2-amine, **3**; MW 218 utilizing pyridine–pyrimidine as a bis-heteroaryl core structure, which functions as both a Cd^{2+} coordination site and a fluorophore. Compound **3** showed sensitive sensing ability toward Cd^{2+} and could successfully discriminate Cd^{2+} from other ions. Furthermore, fluorescence imaging study indicated compound **3** had good cell membrane permeability to apply for a cellular system.

Experimental

Materials and instruments

All chemicals were of the highest purity available. ^{1}H and ^{13}C NMR spectra were recorded on *Varian Gemini 300 and JEOL ECP-400 NMR systems, and the* chemical shifts are reported in ppm. Mass spectra (MS) and HRMS were performed using a JMS-700 spectrometer (JEOL, Tokyo, Japan). UV-Vis absorption spectra were recorded using a UV-Vis spectrophotometer (Shimadzu, Kyoto, Japan). Fluorescence spectra were collected using on a fluorescence spectrophotometer (RF-5300PC, Shimadzu, Kyoto, Japan).

Synthesis of 4-(methylsulfanyl)-6-(pyridin-2-yl)pyrimidin-2-amine (3)

To a solution of 3,3-bis(methylsulfanyl)-1-(pyridin-2-yl)prop-2-en-1-one (**1**) (225 mg, 1 mmol) [26] in pyridine (5 mL), guanidine carbonate (**2**) (270 mg, 1.5 mmol) was added and the mixture was refluxed for 5 h. The reaction mixture was poured into 100 mL of ice water, and the precipitate was collected by filtration, washed with water, and dried overnight. The product was recrystallized from methanol to give **3** (64 g, 29% yield) as pale-yellow crystals. Mp 142–143 °C. ^{1}H-NMR ($CDCl_3$, 300 MHz) δ 2.54 (s, 3H), 5.14 (brs, 2H), 7.32 (dd, *J* = 1.2, 7.5 Hz, 1H), 7.55 (s, 1H), 7.77 (dd, *J* = 1.8, 7.5 Hz, 1H), 8.26 (d, *J* = 7.8 Hz, 1H), 8.65 (d, *J* = 4.8, Hz, 1H). ^{13}C NMR ($CDCl_3$, 75 MHz) δ 12.9, 105.2, 121.9, 125.1, 137.1, 149.5, 154.5, 162.1, 162.5, 173.1. MS m/z: 219 [M + H^+]. HRMS calcd for $C_{10}H_{11}N_4S$ [M + H^+]: 219.0704. Found: 219.0695.

Synthesis of 4-(methylsulfanyl)-6-phenylpyrimidin-2-amine (5)

Compound **5** was prepared from 3,3-bis(methylsulfanyl)-1-phenylprop-2-en-1-one (**4**, 224 mg, 1.0 mmol) and guanidine carbonate (**2**) (270 mg, 1.5 mmol) in a manner similar to that described for the synthesis of **3**. Recrystallization from methanol gave **5** (68 mg, 31% yield) as pale-yellow crystals (mp 97–98 °C). ^{1}H-NMR ($CDCl_3$, 400 MHz) δ 2.52 (s, 3H), 6.65 (s, 2H), 7.03 (s, 1H), 7.46-7.50 (m, 3H), 8.06 (d, *J* = 7.6 Hz, 2H). MS m/z: 217 [M^+]. HRMS calcd for $C_{11}H_{11}N_3S$ [M^+]: 217.0674. Found: 217.0666.

Synthesis of 4-(pyridin-2-yl)pyrimidin-2-amine (7) [27]

After dissolving sodium (500 mg, 21.8 mmol) in a solution of guanidine carbonate (**2**) (1350 mg, 7.5 mmol) in dry ethanol (10 mL), 3-(dimethylamino)-1-(2-pyridyl)-2-propen-1-one (**6**) (880 mg, 5 mmol) was added, and the mixture was refluxed for 24 h. The reaction mixture was concentrated under reduced pressure, and the residue was recrystallized from methanol to give **7** (770 mg, 44% yield) as pale-yellow crystals (mp 136–137 °C). ^{1}H-NMR ($CDCl_3$, 300 MHz) δ 5.43 (brs, 2H), 7.33 (dd, *J* = 1.2, 7.5 Hz, 1H), 7.60 (d, *J* = 5.1 Hz, 1H), 7.76 (dd, *J* = 1.8, 6.0 Hz, 1H), 8.28 (d, *J* = 7.8 Hz, 1H), 8.41 (d, *J* = 5.1 Hz, 1H), 8.67 (d, *J* = 6.0 Hz, 1H). ^{13}C NMR ($CDCl_3$, 75 MHz) δ 108.2, 121.7, 125.3, 137.1, 149.6, 154.6, 159.5, 163.4, 164.3. MS m/z: 173 [M + H^+]. HRMS calcd for $C_9H_9N_4$ [M + H^+]: 173.0827. Found: 173.0822.

Spectroscopic studies

A stock solution of each compound (1×10^{-2} mol L^{-1}) was prepared in DMSO. Solutions of metal ions were prepared by dissolving the perchlorate salts of metal ions (Na^+, K^+, Mg^{2+}, Ca^{2+}, Fe^{2+}, Fe^{3+}, Ni^{2+}, Zn^{2+}, Cd^{2+}, Co^{2+}, Cu^{2+}, Mn^{2+}, and Al^{3+}) in deionized water. The fluorescence of each compound (10^{-6} mol L^{-1}) was analyzed in the absence and presence of metal ions in EtOH/H_2O (1:1, v/v). A Job' plot was used to investigate the binding stoichiometry of **3** to Cd^{2+}. The dissociation constant (K_d) was determined from a Benesi–Hidebrand plot [28,29].

$$1/(F - F_0) = 1/\{K_a(F_{max} - F_0)[Zn^{2+}]^n\} + 1/(F_{max} - F_0)$$

where F, F_0, and F_{max} are the fluorescence intensity, the fluorescence intensity without Cd^{2+}, and the fluorescence intensity in the presence of excess Cd^{2+}, respectively. The association constant (K_a) (the inverse of K_d) was determined from the slope of the plot of $1/(F - F_0)$ against $1/[Cd^{2+}]$. The selectivity of **3** for Cd^{2+} was investigated using 10^{-2} mol L^{-1} metal cation solutions. The effect of pH on the fluorescence properties of **3** was evaluated using various buffers: *tris(hydroxymethyl)aminomethane hydrochloride* buffer (pH 3.0), acetate buffer (pH 4.0–5.0), and tris-hydrochloric acid buffer (pH 6.0–8.0).

Cellular imaging using fluorescence microscope

Mouse macrophage-like cells (RAW264) were cultured in Dulbecco's modified Eagle's medium that included 10% fetal bovine serum and 1% penicillin at 37 °C in a humidified atmosphere with 5% CO_2. The

cells were incubated with **3** (100 μmol L^{-1}) in culture media for 30 min at 37 °C. After washing with phosphate-buffered saline (PBS), the treated cells were incubated with $Cd(ClO_4)_2 \cdot 6H_2O$ (300 μmol L^{-1}) in culture media for 30 min at 37 °C. The incubated cells were imaged using a fluorescence microscope BZ-X710 (Keyence, Osaka, Japan).

Results And Discussion

Pyridine–pyrimidine compound **3** was synthesized with 29% yield via the one-pot reaction of 3,3-bis(methylsulfanyl)-1-(pyridin-2-yl)prop-2-en-1-one (**1**) and guanidine carbonate (**2**) in pyridine (Scheme 1).

The UV-Vis absorption spectra of **3** in EtOH/H_2O (1:1, v/v) were recorded during titration with Cd^{2+} (Fig. 1). The addition of Cd^{2+} altered the absorption spectrum of **3** in a Cd^{2+}-concentration-dependent manner. Specifically, the absorption peaks at wavelengths 260 and 350 nm of **3** gradually increased with increasing amounts of Cd^{2+}. Fig. 2 shows the course of the fluorescence titration of **3** with Cd^{2+} in EtOH/H_2O (1:1, v/v). Free compound **3** showed fluorescence centered at 412 nm upon excitation at 334 nm. With the addition of Cd^{2+}, the fluorescence intensity gradually increased in a Cd^{2+}-concentration-dependent manner and the emission maximum wavelength of **3** exhibited a bathochromic shift of 8 nm, indicating that a CHEF effect occurred with Cd^{2+}. Job' plot analysis revealed that the complex formed between compound **3** and Cd^{2+} had a 1:1 stoichiometry (Fig. S1). The dissociation constant (K_d) of this complex, as derived from the fluorescence titration data using Benesi–Hildebrand equation [28,29], was 5.4 x 10^{-6} mol L^{-1} (Fig. S2). In addition, the limit of detection (LOD) of **3**, calculated using LOD = 3σ/slope, was 4.4 × 10^{-7} mol L^{-1}. Thus, the sensitivity of compound **3** is comparable to or better than those of other reported Cd^{2+} fluorescence probes.

The selectivity of **3** for Cd^{2+} detection was evaluated by fluorescence spectrometry in the presence of various cations (Al^{3+}, Ca^{2+}, Co^{2+}, Cu^{2+}, Fe^{2+}, Fe^{3+}, K^+, Mg^{2+}, Mn^{2+}, Na^+, Ni^{2+}, and Zn^{2+}) in EtOH/H_2O (1:1, v/v). As shown in Fig. 3, the fluorescence turn-on response was only observed when Cd^{2+} was added to the solution of **3**. Upon the addition of Zn^{2+}, no fluorescence enhancement was observed, indicating that compound **3** could completely discriminate Cd^{2+} from Zn^{2+}. Furthermore, biologically relevant ions such as alkali ions (Na^+ and K^+) and group 2 ions (Ca^{2+} and Mg^{2+}) existing in the millimolar range in living systems had insignificant effects on the fluorescence spectrum of **3**. In the presence of heavy metal ions (Co^{2+}, Cu^{2+}, Fe^{2+}, Fe^{3+}, Mn^{2+}, and Ni^{2+}) and Al^{3+}, the emission maximum peak showed a bathochromic shift of approximately 10 nm and fluorescence quenching was observed. We also carried out competition experiments between Cd^{2+} and other cations (Fig. 4). After the addition of each metal ion (Al^{3+}, Ca^{2+}, Co^{2+}, Cu^{2+}, Fe^{2+}, Fe^{3+}, K^+, Mg^{2+}, Mn^{2+}, Na^+, Ni^{2+}, and Zn^{2+}) to the solution of **3**, the same amount of Cd^{2+} was added. Fluorescence quenching was observed in the presence of some heavy metal ions including Ni^{2+}, Cu^{2+}, and Fe^{3+}, indicating that these metal ions interfere with the binding of Cd^{2+} to **3**. In the presence of other metal ions including alkali ions (Na^+ and K^+), group 2 ions (Ca^{2+} and Mg^{2+}) and Zn^{2+},

CHEF effects were observed with Cd^{2+}. Although fluorescence quenching was observed with Fe^{2+}, Co^{2+}, Mn^{2+}, and Al^{3+}, the fluorescence intensity increased again upon adding Cd^{2+}, indicating that these metals were displaced by Cd^{2+}. These spectroscopic data indicated that compound **3** could be a selective probe for Cd^{2+}.

The Cd^{2+} selectivity of compound **3** was investigated using analogs **5** and **7**, which are closely related to **3**. As shown in Scheme 2, benzene–pyrimidine analog **5** without a terminal basic nitrogen and demethylsulfanyl analog **7** were prepared with 31% and 41% yields, respectively. Spectroscopic studies (Fig. 5) revealed that benzene–pyrimidine analog **5** did not show a turn-on response to Cd^{2+}, likely due to the lack of a coordination site. Thus, the interaction of **3** with Cd^{2+} involves the pyridine–pyrimidine moiety. Furthermore, demethylsulfanyl analog **7** exhibited bathochromic shift of 10 nm upon adding both Cd^{2+} and Zn^{2+}, indicating that the methylsulfanyl group at the 4-position of the pyrimidine ring affects the ICT state and Cd^{2+} selectivity. Based on this result, we will develop related compounds with different substituents at the 4-position of the pyrimidine ring in the future.

To evaluate the influence of pH on the Cd^{2+} detecting ability of **3**, we measured the intensity at the fluorescent maximum wavelength (415 nm) in buffer solutions at different pH ranges in the absence and presence of Cd^{2+} (Fig. 6). The fluorescence of **3** at pH 3 decreased in the absence of Cd^{2+} owing to the disruption of **3**-Cd^{2+} complex formation by the protonation of the nitrogen atom of free **3**. However, the fluorescence intensities of **3** in the absence and presence of Cd^{2+} were nearly constant in the range of pH 4–8. These results indicate that compound **3** can function as a Cd^{2+} probe under physiological conditions. Thus, we studied compound **3** via cellular imaging to evaluate its cell membrane permeability.

Fig. 7 shows the fluorescence microscopy images of living cells (mouse macrophage-like cells; RAW264). The cells cultured in the Dulbecco's modified Eagle's medium was incubated with **3** (100 μmol L^{-1}) for 30 min at 37 °C in a humidified atmosphere of 5% CO_2. After the cells were washed with PBS to remove excess of **3**, they exhibited a very weak fluorescence signal [Fig. 7(a)]. In contrast, the cells treated with **3** (100 μmol L^{-1}) for 30 min and Cd^{2+} (300 μmol L^{-1}) for another 30 min showed a bright intracellular fluorescence signal [Fig. 7(b)]. These data indicate that compound **3** has good cell membrane permeability and a fluorescence turn-on response to intracellular Cd^{2+}. In addition, no significant cytotoxicity was observed during this study.

Conclusion

To develop a Cd^{2+} selective fluorescence probe with cell membrane permeability, we synthesized low-molecular-weight **3** (MW = 218) based on pyridine-pyrimidine as a bis-heterocyclic core structure from the one-pot synthesis of 3,3-bis(methylsulfanyl)-1-(pyridin-2-yl)prop-2-en-1-one with guanidine carbonate in pyridine and evaluated its fluorescence properties. Compound **3** could successfully discriminate between Cd^{2+} from Zn^{2+}, and showed a Cd^{2+}-selective fluorescence turn-on response in the presence of other biologically relevant metal ions. Moreover, fluorescence imaging of living cells showed that the cell

membrane permeability of compound **3** is sufficient to respond to intracellular Cd^{2+}. Thus, we expect that compound **3,** as a novel low-molecular-weight fluorescence probe for Cd^{2+} will contribute to the selective detection and investigation of cadmium in biological and environmental systems.

Declarations

Authors' Contributions All the authors (M. Hagimori, Y. Karimine, N. Mizuyama, F. Hara, T. Fujino, H. Saji, T. Mukai) made substantial contribution while preparing the manuscript.

Funding This work was partly supported by the Konica Minolta Imaging Science Encouragement Award of Konica Minolta Science and Technology Foundation.

Data Availability The data used to support the findings of this study are included within the article.

Compliance with Ethical Standards

Conflict of Interest The authors declare that they have no conflict of interest.

Code Availability Not applicable.

References

1. Satarug S, Vesey DA, Gobe GC (2017) Current health risk assessment practice for dietary cadmium: Data from different countries. Food Chem Toxicol 106: 430–445
2. Shahid M, Dumat C, Khalid S, Niazi NK, Antunes PMC (2017) Cadmium bioavailability, uptake, toxicity and detoxification in soil-plant system. Rev Environ Contam Toxicol 241: 73–137
3. Genchi G, Sinicropi MS, Lauria G, Carocci A, Catalano A (2020) The Effects of cadmium toxicity. Int J Environ Res Public Health 17: 3782
4. Wang B, Du Y. Cadmium and its neurotoxic effects (2013) Oxid Med Cell Longev 2013: 898034
5. Kundu S, Sengupta S, Chatterjee S, Mitra S, Bhattacharyya A (2009) Cadmium induces lung inflammation independent of lung cell proliferation: A molecular approach. J Inflamm (Lond) 6: 19
6. Jarup L, Akesson A (2009) Current status of cadmium as an environmental health problem. Toxicol Appl Pharmacol 238: 201–208
7. Song JK, Luo H, Yin XH, Huang GL, Luo SY, Lin DR, Yuan DB, Zhang W, Zhu JG (2015) Association between cadmium exposure and renal cancer risk: a meta-analysis of observational studies. Sci Rep 11: 17976
8. Goyer RA, Liu J, Waalkes MP (2004) Cadmium and cancer of prostate and testis. Biometals 17: 555–558
9. Kaya G, Yaman M (2008) Online preconcentration for the determination of lead, cadmium and copper by slotted tube atom trap (STAT)-flame atomic absorption spectrometry. Talanta 75: 1127–1133

10. Davis AC, Calloway CP, Jones BT (2007) Direct determination of cadmium in urine by tungsten-coil inductively coupled plasma atomic emission spectrometry using palladium as a permanent modifier. Talanta 71: 1144–1149
11. Wu D, Chen L, Lee W, Ko G, Yin J, Yoon J (2018) Recent progress in the development of organic dye based near-infrared fluorescence probes for metal ions. Coord Chem Rev 354: 74–79
12. Carter KP, Young AM, Palmer AE (2014) Fluorescent sensors for measuring metal ions in living systems. Chem Rev 114: 4564–4601
13. Prodi L, Montalti M, Zaccheroni N, Bradshaw JS, Izatt RM, Savage PB (2001) Characterization of 5-chloro-8-methoxyquinoline appended diaza-18-crown-6 as a chemosensor for cadmium. Tetrahedron Lett 42: 2941–2944
14. Yuasa H, Miyagawa N, Izumi T, Nakatani M, Izumi M, Hashimoto H (2004) Hinge sugar as a movable component of an excimer fluorescence sensor. Org Lett 6: 1489–1492
15. Xue L, Li G, Liu Q, Wang H, Liu C, Ding X, He S, Jiang H (2011) Ratiometric fluorescent sensor based on inhibition of resonance for detection of cadmium in aqueous solution and living cells. Inorg Chem 50: 3680–3690
16. Avirah RR, Jyothish K, Ramaiah D (2008) Infrared absorbing croconaine dyes: Synthesis and metal ion binding properties. J Org Chem 73: 274–279
17. Zhang T, Guo X, Zheng M, Yang R, Yang H, Jia L, Yang M (2017) A 4,5-quinolimide-based fluorescent sensor for the turn-on detection of Cd^{2+} with live-cell imaging. Org Biomol Chem 15: 2211–2216
18. Taki M, Desaki M, Ojida A, Iyoshi S, Hirayama T, Hamachi I, Yamamoto Y (2008) Fluorescence imaging of intracellular cadmium using a dual-excitation ratiometric chemosensor. J Am Chem Soc 130: 12564–12565
19. Côrte-Real L, Teixeira RG, Girio P, Comsa E, Moreno A, Nasr R, Baubichon-Cortay H, Avecilla F, Marques F, Robalo MP, Mendes P, Ramalho JPP, Garcia MH, Falson P, Valente A (2018) Methyl-cyclopentadienyl ruthenium compounds with 2,2'-bipyridine derivatives display strong anticancer activity and multidrug resistance potential. Inorg Chem 57: 4629–4639
20. Ajayaghosh A, Carol P, Sreejith S (2005) A ratiometric fluorescence probe for selective visual sensing of Zn^{2+}. J Am Chem Soc 127: 14962–14963
21. Jiang X, Park BG, Riddle JA, Zhang BJ, Pink M, Lee D (2008) Torsionally restricted tetradentate fluorophore: a swivelling ligand platform for ratiometric sensing of metal ions. Chem Commun: 6028–6030
22. Maity D, Govindaraju T (2010) Pyrrolidine constrained bipyridyl-dansyl click fluoroionophore as selective Al^{3+} sensor. Chem Commun 46: 4499–4501
23. Hagimori M, Temma T, Mizuyama N, Uto T, Yamaguchi Y, Tominaga Y, Mukai T, Saji H (2015) A high-affinity fluorescent Zn^{2+} sensor improved by the suppression of pyridine-pyridone tautomerism and its application in living cells. Sens Act B Chem 213: 45–52

24. Hagimori M, Mizuyama N, Tominaga Y, Mukai T, Saji H (2015) A low-molecular-weight fluorescent sensor with Zn^{2+} dependent bathochromic shift of mission wavelength and its imaging in living cells. Dyes Pigm 113: 205–209
25. Hagimori M, Taniura M, Mizuyama N, Karimine Y, Kawakami S, Saji H, Mukai T (2019) Synthesis of a novel pyrazine–pyridone biheteroaryl-based fluorescence sensor and detection of endogenous labile zinc ions in lung cancer cells. Sensors 19: 2049–2059
26. Mizuyama N, Kohra S, Ueda K, Hiraoka K, Takahashi K, Tominaga Y (2007) Synthesis and fluorescence of 4-methylsulfanyl-6-pyridyl-2H-pyran-2-ones in solid state. Heterocycles 71: 399–409
27. Ghoochany LT, Kerner C, Farsadpour S, Menges F, Sun Y, Niedner-Schatteburg G, Thiel WR (2013) C-H activation at a ruthenium(II) complex - The Key step for a base-free catalytic transfer hydrogenation?. Euro J Inorg Chem 2013: 4305–4317
28. Benesi HA, Hildebrand JH (1949) A spectrophotometric investigation of the interaction of iodine with aromatic hydrocarbons. J Am Chem Soc 71: 2703–2707
29. Kumawat LM, Asif M, Gupta VK (2017) Dual ion selective fluorescence sensor with potential applications in sample monitoring and membrane sensing. Sens Act B Chem 241: 1090–1098

Schemes

Scheme 1 and 2 are available in the Supplementary Files.

Figures

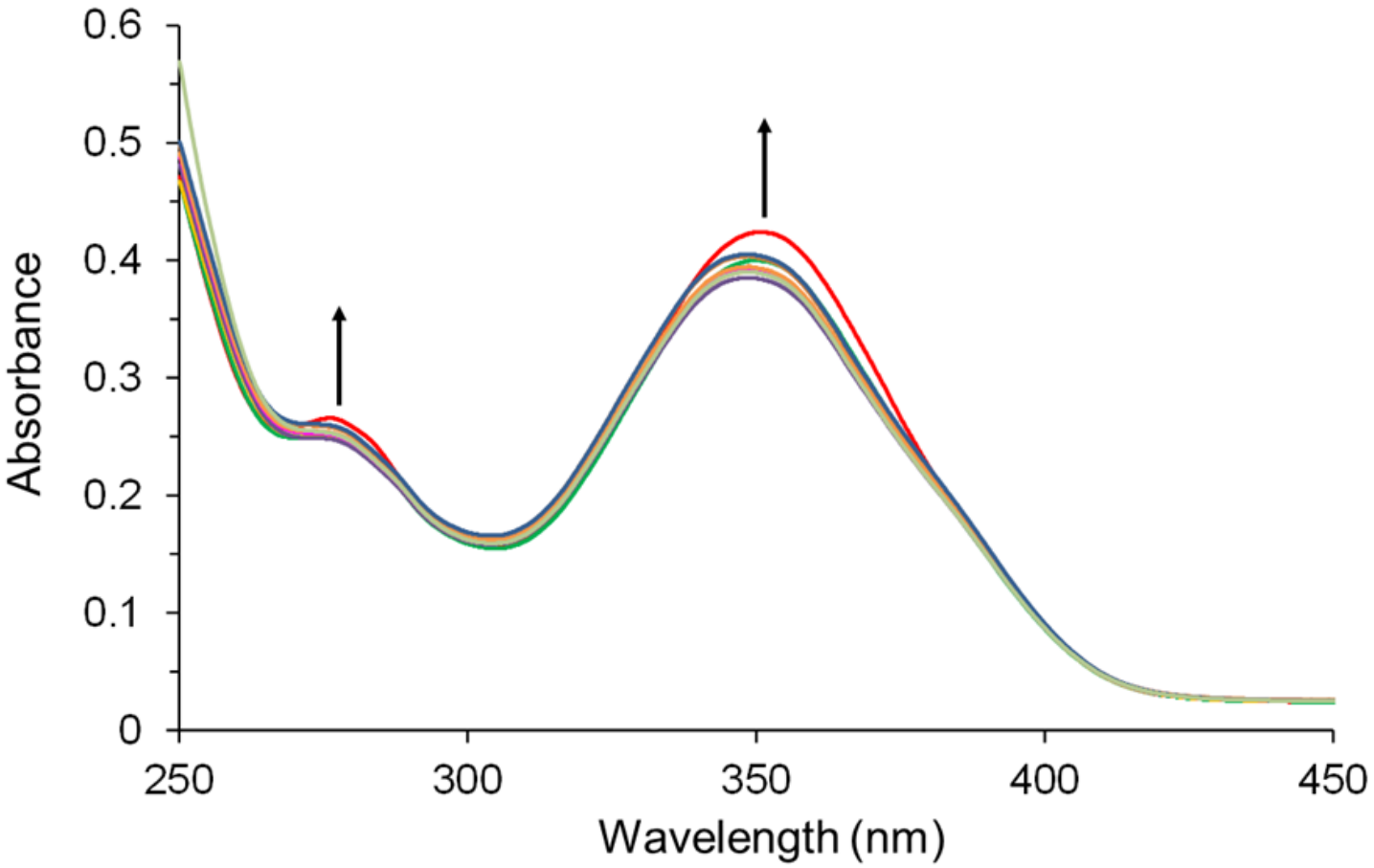

Figure 1

Changes in the UV-Vis absorption of 3 (10−5 mol L−1) upon the addition of Cd2+ (0–100 μmol L-1) in EtOH/H2O (1:1, v/v)

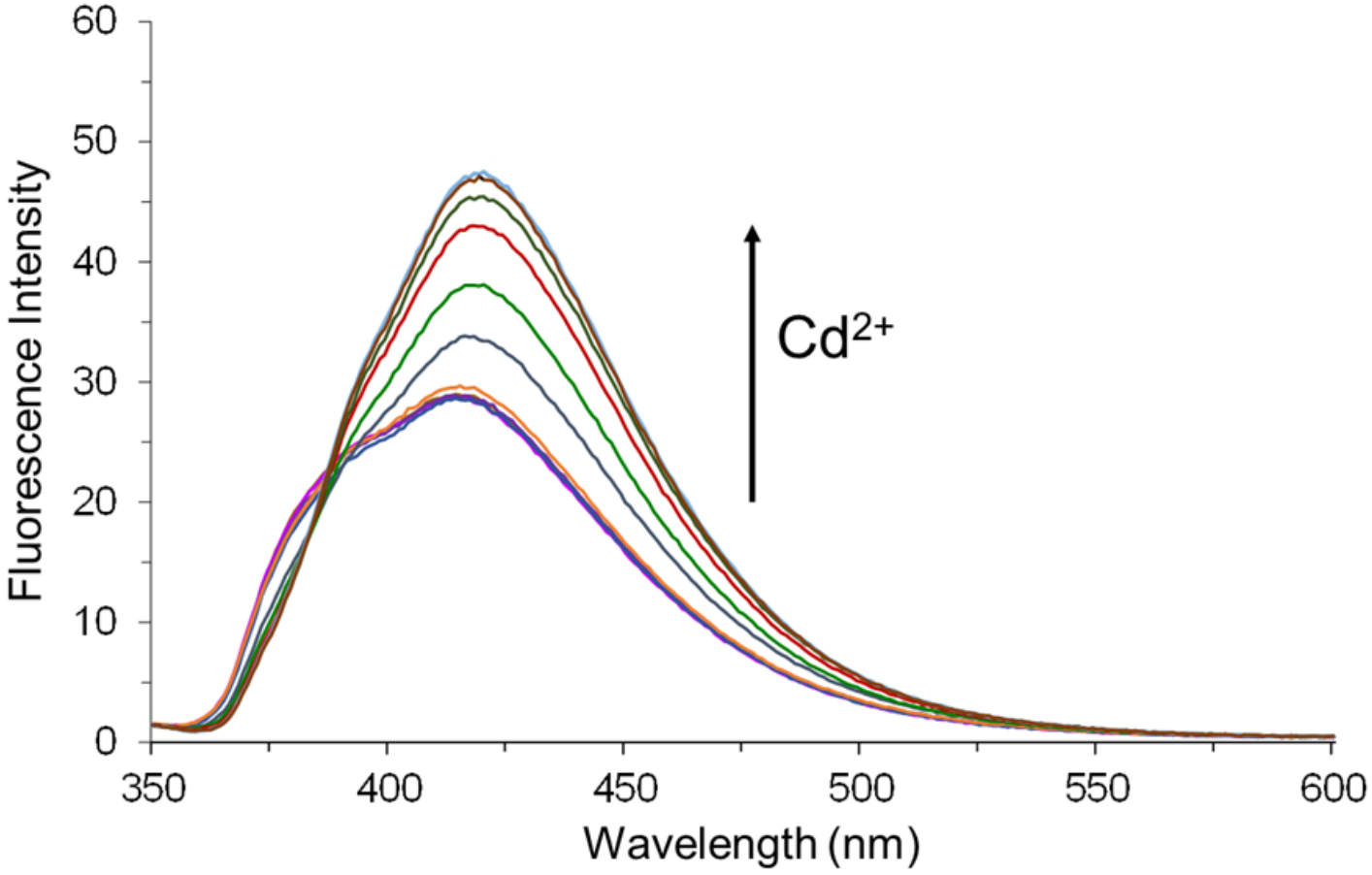

Figure 2

Changes in the fluorescence of 3 (10−6 mol L−1) upon the addition of Cd2+ (0–100 μmol L−1) in EtOH/H2O (1:1, v/v); excitation wavelength: 334 nm.

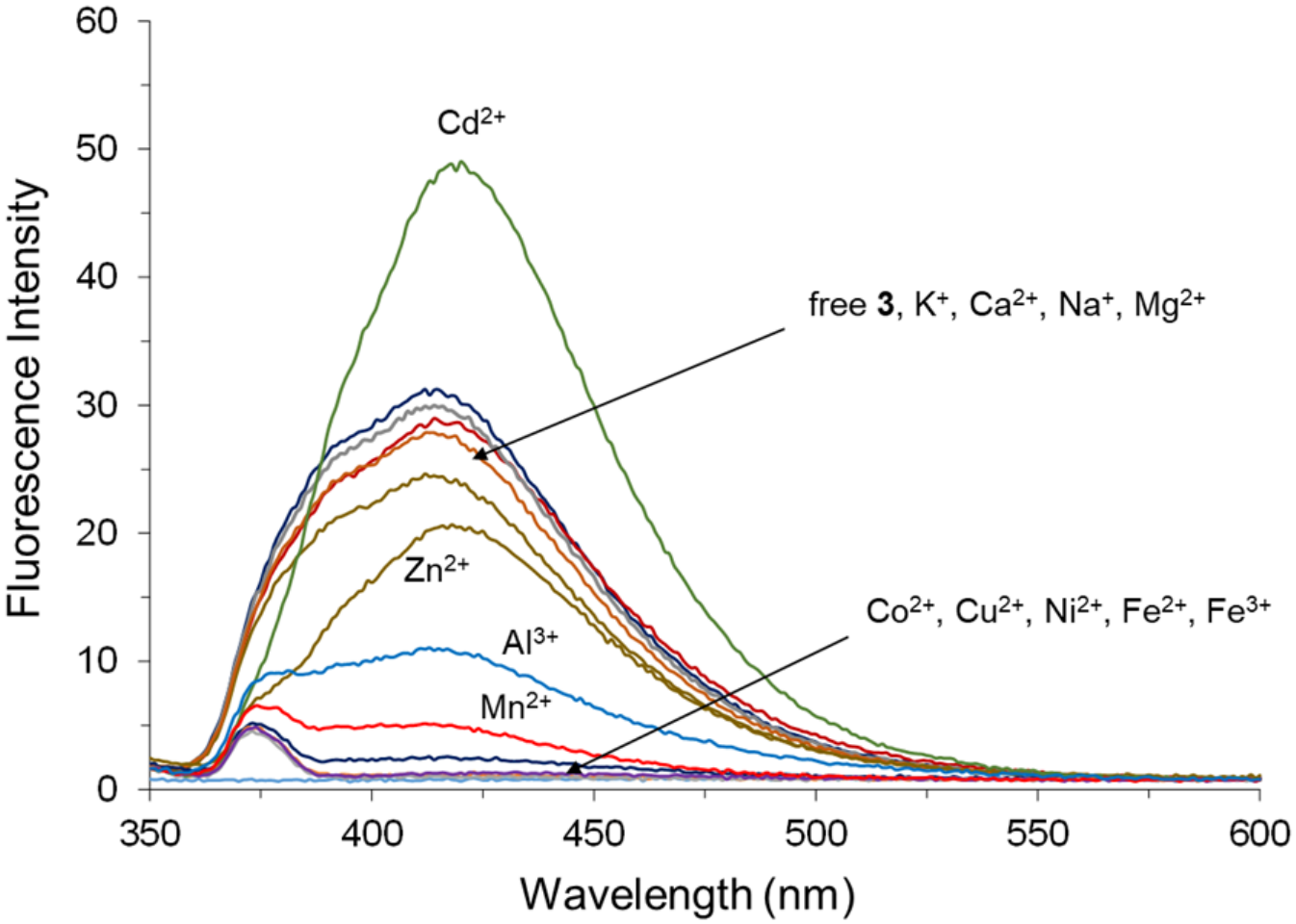

Figure 3

Fluorescence spectra of 3 (10−6 μmol L−1) and various metal cations (100 μmol L−1) in EtOH/H2O (1:1, v/v); excitation wavelength: 334 nm).

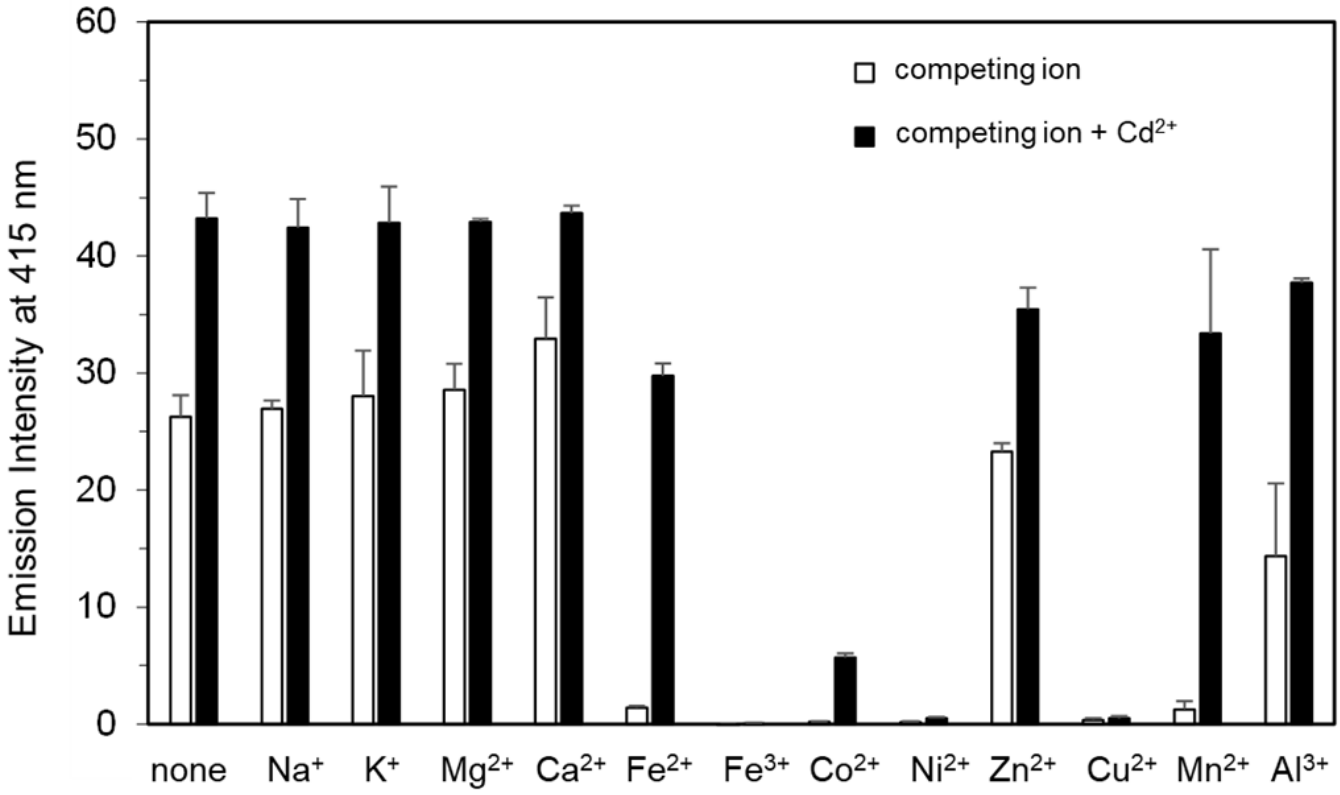

Figure 4

Competitive binding experiments between various metal ions (10−3 mol L−1) and Cd2+ (10−3 mol L−1) with 3 (10−6 mol L−1) in EtOH/H2O (1:1, v/v); excitation wavelength: 334 nm.

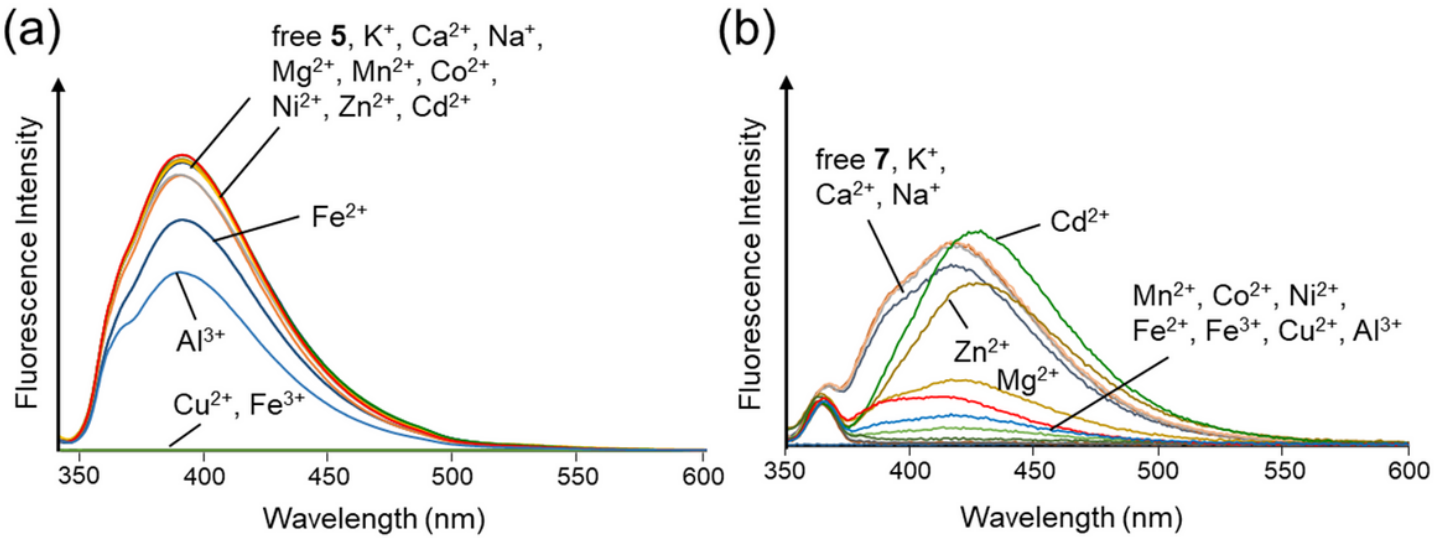

Figure 5

Fluorescence spectra of (a) 5 (excitation wavelength: 324 nm) and (b) 7 (excitation wavelength: 346 nm) upon addition of metal cations in EtOH/H2O (1:1, v/v)

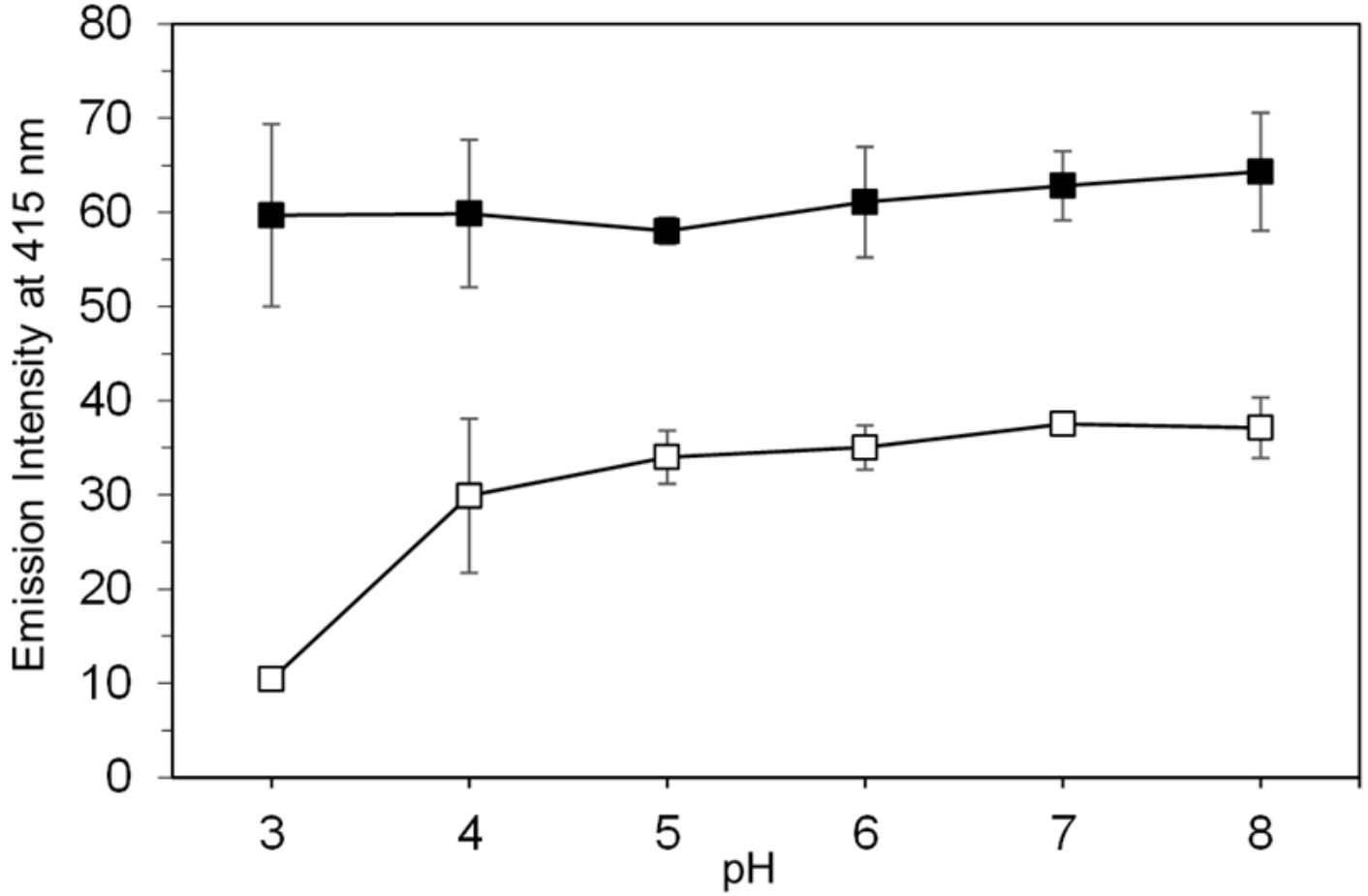

Figure 6

Effect of pH on the fluorescence intensity of 3 in the absence (□) and presence (■) of Cd2+

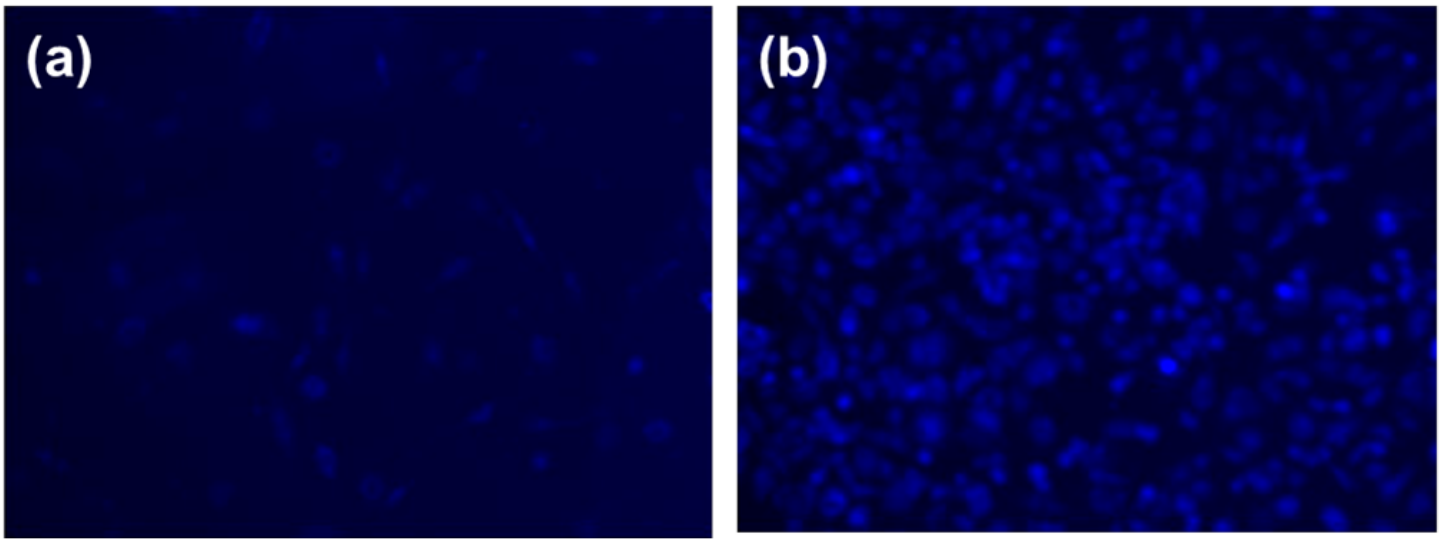

Figure 7

Fluorescence microscopy images of RAW 264 cells. (a) treated with 3 (100 μmol L−1) only and (b) treated with both 3 (100 μmol L−1) and Cd2+ (300 μmol L−1)

Supplementary Files

This is a list of supplementary files associated with this preprint. Click to download.

- Scheme1.png
- Scheme2.png